Journal of Engineering Mathematics **44:** 155–171, 2002.

Microwave heating in multiphase systems: evaluation of series solutions

K. G. AYAPPA and TIRTHANKAR SENGUPTA
Department of Chemical Engineering Indian Institute of Science, Bangalore - 560012 INDIA

Received 25 January 2002; accepted in revised form 3 June 2002

Abstract. The 1D electric field and heat-conduction equations are solved for a slab where the dielectric properties vary spatially in the sample. Series solutions to the electric field are obtained for systems where the spatial variation in the dielectric properties can be expressed as polynomials. The series solution is used to obtain electric-field distributions for a binary oil-water system where the dielectric properties are assumed to vary linearly within the sample. Using the finite-element method temperature distributions are computed in a three-phase oil, water and rock system where the dielectric properties vary due to the changing oil saturation in the rock. Temperature distributions predicted using a linear variation in the dielectric properties are compared with those obtained using the exact nonlinear variation.

Key words: microwaves, oil recovery, porous media, series solutions

1. Introduction

Electromagnetic radiation with frequencies ranging between 300 MHz to 300 GHz are referred to as microwave radiation. Applications where microwave energy is used range from more common applications such as heating and thawing of food to more specialized materials processing situations such as ceramic sintering. Recently there has been much debate about the potential uses of electromagnetic energy for decontamination of soils and enhanced oil recovery. In the case of oil recovery preheating the oil-bearing rock formation would potentially lower the oil viscosity and enhance the production of oil [1]. An alternate method is to radiate the water while the displacement process occurs in the oil-bearing formation [2]. The heated water would then transfer heat to the oil, thereby enhancing its recovery.

During immiscible displacement, where water is used to displace oil in a porous rock, a front is established [3, Chapter 6]. The front is usually characterized by the oil saturation which varies in a nonlinear fashion from a region of pure water to a region of pure oil as shown schematically in Figure 1. We are interested in studying the microwave heating of an oil-water mixture contained in a porous rock formation after the displacement front has been established. Microwaves are assumed to be incident from the water side as shown in Figure 1. A complete model would involve the microwave source and the computational domain would then include the water, oil-water and oil regions as shown in Figure 2. In this manuscript we will analyze the single-layer situation shown in Figure 1 where the porous slab containing oil and water is placed in free space. Once the front is established, the dielectric properties of the oil-water region are spatially dependent functions, where the functional dependence is due to the changing oil saturation in the medium. We will illustrate that the problem reduces to solving the electric-field equation with spatially varying coefficients. We develop series solutions for the electric field, assuming that the dielectric properties can be expressed as

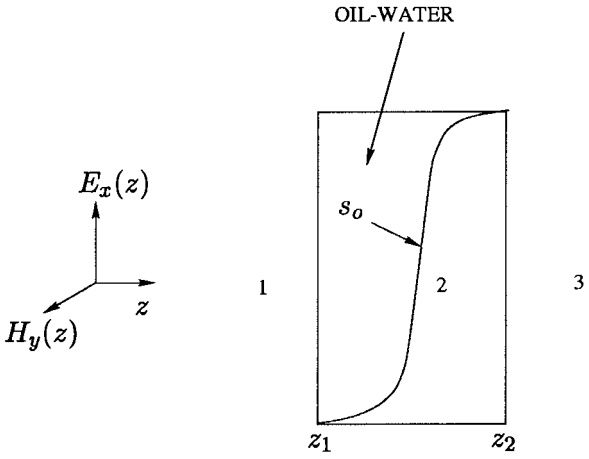

Figure 1. Schematic of single-layer system, where the medium 2 is a porous rock containing oil and water. $0 \leq s_o \leq 1$, the saturation of oil is shown as well.

polynomials that span the domain. We test the series solutions with a finite-element solution for different sample thicknesses. Temperature distributions are obtained by use of the exact functional forms for the spatial variation of dielectric properties in the three-phase oil, water and rock system and compared with the heating patterns with the assumption of a linear variation in the dielectric properties, for which the series solution can be used. In addition to studying heating patterns in the single layer situation, we also present solutions to the electric field for the multilayer situation depicted in Figure 2.

2. Theory

2.1. Electric-field equations

Consider a slab exposed to transverse electromagnetic radiation as shown in Figure 1. We are interested in studying the microwave power absorption and subsequent heating in the region $Z_1 \leq Z \leq Z_2$, which is made up of a porous medium, within which the saturation of oil s_o varies spatially as shown in Figure 1. As a result, the dielectric properties of the medium vary in the region $Z_1 \leq Z \leq Z_2$, due to the spatial variation in the water saturation s_w. The saturation shown depicted in Figure 1 depicts the region around the water-oil front that is established when water is used to displace oil from the formation. The saturation s_o is defined as the volume fraction of pore space occupied with oil. Hence the water saturation $s_w = 1 - s_o$. Since oil is present in the rock formations over geological time scales, we assume that rock is oil-wet, and oil forms the continuous phase in the two-phase oil-water system. We further make the assumption of a quasi-steady state and study the electric field and temperature distribution across a stationery oil-water front.

Let k_1, $k_2(Z)$ and k_3 represent the propagation constants in regions 1, 2 and 3, respectively (Figure 1). Assuming that the incident radiation is a uniform plane wave, whose electric and magnetic components lie in a plane $(x - y)$ of uniform intensity varying only in the direction of propagation (Z), the equation for the electric field E_{x2} (assuming a time harmonic form $e^{i\omega t}$) is

$$\frac{\mathrm{d}^2 E_{x2}}{\mathrm{d}Z^2} + k_2^2(Z) E_{x2} = 0, \qquad Z_1 \le Z \le Z_2, \tag{1}$$

where the propagation constant

$$k_2^2 = \frac{\omega^2}{c^2}[\kappa_2'(s_o(Z)) + \mathrm{i}\kappa_2''(s_o(Z))] \tag{2}$$

is dependent on the spatially varying dielectric properties, κ', the relative dielectric constant and κ'', the relative dielectric loss. Here $\omega = 2\pi f$, where f is the frequency of the electromagnetic radiation and c is the velocity of light. An equivalent expression for the propagation constant is

$$k_2 = 2\pi/\lambda_{m2} + \mathrm{i}/D_{p2}, \tag{3}$$

where the wavelength of radiation in medium 2,

$$\lambda_{m2} = \frac{\lambda_0}{\sqrt{\frac{\kappa_2'}{2}}\sqrt{\sqrt{1+\left(\frac{\kappa_2''}{\kappa_2'}\right)^2}+1}}, \tag{4}$$

and the penetration depth

$$D_{p2} = \frac{\lambda_0}{\pi\sqrt{2\kappa_2'}\sqrt{\sqrt{1+\left(\frac{\kappa_2''}{\kappa_2'}\right)^2}-1}} \tag{5}$$

In Equations (4) and (5), $\lambda_0 = c/f$ the free-space wavelength. Equation (3) is useful as it relates the propagation constant to length scales that are important in electromagnetic heating applications.

Since the dielectric properties in regions 1 and 2 are spatially invariant, we seek boundary conditions at $Z = Z_1$ and $Z = Z_2$. Assuming a wave propagating in the positive Z direction, we have the electric field in region 1:

$$E_{x1} = E_0 \mathrm{e}^{\mathrm{i}k_1 Z} + A\mathrm{e}^{-\mathrm{i}k_1 Z}, \tag{6}$$

and in region 3:

$$E_{x3} = B\mathrm{e}^{\mathrm{i}k_3 Z}. \tag{7}$$

The boundary conditions are obtained by evaluating the field at the required boundary and taking a spatial derivative of the field [4]. Using this procedure, we have the boundary conditions

$$\frac{\mathrm{d}E_{x2}}{\mathrm{d}Z} + \mathrm{i}k_1 E_{x2} = 2\mathrm{i}k_1 E_0 \mathrm{e}^{ik_1 Z_1} \qquad \text{at} \qquad Z = Z_1 \tag{8}$$

and

$$\frac{\mathrm{d}E_{x2}}{\mathrm{d}Z} - \mathrm{i}k_3 E_{x2} = 0 \qquad \text{at} \qquad Z = Z_2. \tag{9}$$

The above boundary conditions are consistent with the continuity of the electric field and its spatial derivatives at the interface. With a knowledge of the electric field intensity in the medium, the local power absorbed in the sample is

$$p(Z) = \frac{1}{2}\omega\epsilon_0\kappa_2''(Z)E_{x2}E_{x2}^* \ , \tag{10}$$

where ϵ_0 is the free-space permittivity and E_{x2}^* is the complex conjugate of the electric field.

The dielectric properties of the porous medium obtained, using the mixture rule for the relative complex dielectric constant $\kappa_2 = \kappa_2' + \mathrm{i}\kappa_2''$ based on a complex conductivity model [5], is

$$\kappa_2 = \frac{\kappa_c\left[\kappa_d\left(1 + s_d V_d\right) + \kappa_c\left(1 - V_d\right)s_d\right]}{\left[\kappa_c\left(s_d + V_d\right) + \kappa_d\left(1 - V_d\right)\right]} \ , \tag{11}$$

where κ_c and κ_d are the relative complex dielectric properties of the continuous and dispersed phases, respectively, s_d = 2 for spherical dispersions and s_d = 1 for cylindrical dispersions. For a two-phase system consisting of oil and water the dielectric properties are obtained assuming that oil is the continuous phase. For the three-phase system of oil, water and rock we first estimate the dielectric properties of the oil-water phase using Equation (11) assuming that oil is the continuous phase. To obtain the dielectric properties of the three-phase system the mixture rule is once again applied with rock as the continuous phase. For the dielectric properties of the oil-water mixture, V_d is the volume fraction of the dispersed phase which is the water saturation $s_w = 1 - s_o$. The functional form of s_o *vs.* Z is

$$s_o = \begin{cases} \dfrac{(Z - Z_1)^2}{(Z_2 - Z_1)\,(Z_m - Z_1)}, & Z_1 \le Z \le Z_m \\ 1 - \dfrac{(Z - Z_2)^2}{(Z_2 - Z_1)\,(Z_2 - Z_m)}, & Z_m \le Z \le Z_2 \end{cases} \ , \tag{12}$$

where $Z_m = (Z_2 - Z_1)/2$ is the mid-point. The above equation for saturation has the desired sigmoidal form [6] for the oil saturation at an idealized water-oil front [3, Chapter 6].

2.2. Heat transport

Assuming that heat transport occurs primarily by conduction, the unsteady-state heat-transfer equation is,

$$\left(\rho C_p\right)_{\text{eff}} \frac{\partial T}{\partial t} = \frac{\partial}{\partial Z}\left(k_{T,\text{eff}}\frac{\partial T}{\partial Z}\right) + p(Z) \ , \tag{13}$$

where $p(Z)$ is a volumetric source term due to microwave power absorption. Equation (13) is solved to obtain transient temperature profiles for a sample exposed to microwave radiation. If the porosity of the medium is ϕ, then the effective thermal conductivity is given by

$$k_{T,\text{eff}} = \phi[s_o k_{T,o} + (1 - s_o)k_{T,w}] + (1 - \phi)k_{T,s}, \tag{14}$$

where $k_{T,o}$, $k_{T,w}$ and $k_{T,s}$ are the thermal conductivities of the oil, water and solid matrix, respectively. Similarly, the effective specific heat capacity is

$$\left(\rho C_p\right)_{\text{eff}} = \phi[s_o\rho_o C_{po} + (1 - s_o)\rho_w C_{pw}] + (1 - \phi)\rho_s C_{ps}, \tag{15}$$

where ρ_i and C_{pi} represent the density and heat capacity of the ith phase, respectively.

2.3. Dimensionless forms

If the slab thickness $Z_2 - Z_1 = L$ and $Z_1 = 0$, then defining the dimensionless variables

$$u = \frac{E_{x2}}{E_0} \qquad \text{and} \qquad z = \frac{Z}{L}, \tag{16}$$

we may reduce the equation for the electric field, Equation (1),

$$\frac{\mathrm{d}^2 u}{\mathrm{d}z^2} + \gamma_2^2(z)u = 0, \qquad 0 \le z \le 1 \tag{17}$$

We assume that the dielectric properties can be represented as pth-order polynomials of the following form,

$$\kappa_2'(z) = \sum_{j=0}^{p} c_j z^j \qquad \text{and} \qquad \kappa_2''(z) = \sum_{j=0}^{p} d_j z^j, \tag{18}$$

and the propagation constant by

$$\gamma_2^2(z) = \sum_{j=1}^{p} \alpha_j z^j, \tag{19}$$

where $\alpha_j = \frac{L^2\omega^2}{c^2}(c_j + \mathrm{i}d_j)$.

If $\gamma_j = k_j L$, the dimensionless boundary conditions are

$$\frac{\mathrm{d}u}{\mathrm{d}z} + \mathrm{i}\gamma_1 u = 2\mathrm{i}\gamma_1 \qquad \text{at} \qquad z = 0 \tag{20}$$

and

$$\frac{\mathrm{d}u}{\mathrm{d}z} - \mathrm{i}\gamma_3 u = 0 \qquad \text{at} \qquad z = 1. \tag{21}$$

2.4. Series solution

Assume a solution of the form

$$u(z) = \sum_{n=0}^{\infty} u_n z^n, \qquad 0 \le z \le 1. \tag{22}$$

The series solution obtained by equating powers in Equation (17) can be expressed as

$$u(z) = u_0 \sum_{n=0}^{\infty} u_{n0} z^n + u_1 \sum_{n=0}^{\infty} u_{n1} z^n, \tag{23}$$

where u_0 and u_1 are two constants to be evaluated by use of the boundary conditions, (20) and (21). The recursion relationships for the coefficients u_{n0} and u_{n1} for polynomials of order $p = 0$, 1, 2 and 3 in Equation (23) are given below:

(a) Constant ($p = 0$): $\gamma_2^2(z) = \alpha_0$:

$$u_{n0} = \frac{-\alpha_0 u_{n-2,0}}{n(n-1)}, \qquad n \ge 2, \tag{24}$$

$$u_{n1} = \frac{-\alpha_0 u_{n-2,1}}{n(n-1)}, \qquad n \ge 2, \tag{25}$$

(b) Linear ($p = 1$) : $\gamma_2^2(z) = \alpha_0 + \alpha_1 z$:

$$u_{n0} = \frac{-\alpha_0 u_{n-2,0} - \alpha_1 u_{n-3,0}}{n(n-1)}, \qquad n \geq 3, \tag{26}$$

$$u_{n1} = \frac{-\alpha_0 u_{n-2,1} - \alpha_1 u_{n-3,1}}{n(n-1)}, \qquad n \geq 3, \tag{27}$$

(c) Quadratic ($p = 2$) : $\gamma_2^2(z) = \alpha_0 + \alpha_1 z + \alpha_2 z^2$:

$$u_{n0} = \frac{-\alpha_0 u_{n-2,0} - \alpha_1 u_{n-3,0} - \alpha_2 u_{n-4,0}}{n(n-1)}, \qquad n \geq 4, \tag{28}$$

$$u_{n1} = \frac{-\alpha_0 u_{n-2,1} - \alpha_1 u_{n-3,1} - \alpha_2 u_{n-4,1}}{n(n-1)}, \qquad n \geq 4, \tag{29}$$

(d) Cubic ($p = 3$) : $\gamma_2^2(z) = \alpha_0 + \alpha_1 z + \alpha_2 z^2 + \alpha_3 z^3$:

$$u_{n0} = \frac{-\alpha_0 u_{n-2,0} - \alpha_1 u_{n-3,0} - \alpha_2 u_{n-4,0} - \alpha_3 u_{n-5,0}}{n(n-1)}, \qquad n \geq 5, \tag{30}$$

$$u_{n1} = \frac{-\alpha_0 u_{n-2,1} - \alpha_1 u_{n-3,1} - \alpha_2 u_{n-4,1} - \alpha_3 u_{n-5,1}}{n(n-1)}, \qquad n \geq 5. \tag{31}$$

In general, the many term recurrence relationship [8, Chapter 23] for a p^{th}-order polynomial is

$$u_{nk} = \sum_{j=0}^{p} \frac{-\alpha_j u_{n-j-2,k}}{n(n-1)}, \qquad n \geq p+2 \qquad \text{and} \qquad k = 0, 1. \tag{32}$$

The coefficients needed to evaluate the coefficients in the above expressions for $p \leq 3$ are

$$u_{00} = 1,\ u_{10} = 0,\ u_{20} = \tfrac{-\alpha_0}{2\cdot 1},\ u_{30} = \tfrac{-\alpha_1}{3\cdot 2},$$

$$u_{01} = 0,\ u_{11} = 1,\ u_{21} = 0, \qquad u_{31} = \tfrac{-\alpha_0}{3\cdot 2}.$$

We next evaluate the constants u_o and u_1 for two different situations shown in Figures 1 and 2.

2.4.1. *Single layer*

Here we assume that the porous slab is surrounded by air on both sides (Figure 1), as a result $\gamma_1 = \gamma_3 = \gamma_0 = \omega^2 L^2/c^2$. The expression for the constants u_0 and u_1 in Equation (22) we obtain using the boundary conditions (20) and (21) are

$$u_0 = \frac{2\mathrm{i}\gamma_0 m_{22}}{\Delta} \qquad \text{and} \qquad u_1 = \frac{-2\mathrm{i}\gamma_0 m_{21}}{\Delta}, \tag{33}$$

where $\Delta = m_{11}m_{22} - m_{12}m_{21}$ with

$$m_{11} = S_0'(0) + \mathrm{i}\gamma_0 S_0(0), \tag{34.1}$$

$$m_{12} = S_1'(0) + \mathrm{i}\gamma_0 S_1(0), \tag{34.2}$$

$$m_{21} = S_0'(1) - \mathrm{i}\gamma_0 S_0(1), \tag{34.3}$$

$$m_{22} = S_1'(1) - \mathrm{i}\gamma_0 S_1(1), \tag{34.4}$$

where

$$S_0 = \sum_{n=0}^{\infty} u_{n0} z^n, \qquad S_1 = \sum_{n=0}^{\infty} u_{n1} z^n \tag{35}$$

and the primes refer to spatial derivatives with respect to z.

For $p = 0$, the constant property situation, the series reduces to a linear combination of sine and cosine functions and the closed-form solution for the electric field is

$$u(z) = A \sin \gamma_2 \, z + B \cos \gamma_2 \, z, \tag{36}$$

where

$$A = \frac{2(\mathrm{i} \tan \gamma_2 - \gamma_{02})}{(\gamma_{20} + \gamma_{02}) \tan \gamma_2 + 2\mathrm{i}} \tag{37.1}$$

$$B = \frac{2(\gamma_{02} \tan \gamma_2 + \mathrm{i})}{(\gamma_{20} + \gamma_{02}) \tan \gamma_2 + 2\mathrm{i}} \tag{37.2}$$

where $\gamma_{ij} = \gamma_i / \gamma_j$

2.4.2. *Multilayer*

Here we analyze the composite medium shown in Figure 2. The expressions for the electric field in three different layers are,

$$u_2(z) = a_2 \mathrm{e}^{\mathrm{i}\gamma_2 z} + b_2 \mathrm{e}^{-\mathrm{i}\gamma_2 z}, \qquad z_1 < z < z_2, \tag{38.1}$$

$$u_3(z) = a_3 S_0(z) + b_3 S_1(z), \qquad z_2 < z < z_3, \tag{38.2}$$

$$u_4(z) = a_4 \mathrm{e}^{\mathrm{i}\gamma_4 z} + b_4 \mathrm{e}^{-\mathrm{i}\gamma_4 z}, \qquad z_3 < z < z_4, \tag{38.3}$$

$u_2(z)$ and $u_4(z)$ are the expressions for the water and oil layers, respectively, and $u_3(z)$ is the series solution for region 3. The boundary condition at $z_1 = 0$ for u_2 is similar to Equation (20) and the boundary condition for u_4 at $z_4 = 1$ is similar to Equation (21) with γ_3 replaced with γ_5.

$$\left.\begin{aligned} u_l &= u_{l+1} \\ \frac{\mathrm{d}u_l}{\mathrm{d}z} &= \frac{\mathrm{d}u_{l+1}}{\mathrm{d}z} \end{aligned}\right\} \qquad \text{at} \qquad z_l; \qquad l = 2, 3. \tag{39}$$

Using the boundary conditions and interface conditions (39) we can express the constants as

$$a_3 = f_1 m_{22} / \Delta, \tag{40.1}$$

$$b_3 = -f_1 m_{21} / \Delta, \tag{40.2}$$

$$a_4 = \frac{u_3(z_3) \mathrm{e}^{-\mathrm{i}\gamma_4 z_3}}{1 + R_{45} \mathrm{e}^{2\mathrm{i}\gamma_4 (1 - z_3)}}, \tag{40.3}$$

$$b_4 = a_4 R_{45} e^{i2\gamma_4}, \tag{40.4}$$

$$a_2 = T_{12} + R_{21} b_2, \tag{40.5}$$

$$b_2 = \frac{u_3(z_2) e^{-i\gamma_2 z_2} - T_{12}}{R_{21} + e^{-2i\gamma_2 z_2}}, \tag{40.6}$$

where

$$\Delta = m_{11} m_{22} - m_{12} m_{21}, \tag{41.1}$$

$$m_{11} = [i\gamma_2 (\frac{R_{21} - e^{-2i\gamma_2 z_2}}{R_{21} + e^{-2i\gamma_2 z_2}}) S_0(z_2) - S_0'(z_2)], \tag{41.2}$$

$$m_{12} = [i\gamma_2 (\frac{R_{21} - e^{-2i\gamma_2 z_2}}{R_{21} + e^{-2i\gamma_2 z_2}}) S_1(z_2) - S_1'(z_2)], \tag{41.3}$$

$$m_{21} = [i\gamma_4 (\frac{1 - R_{45} e^{2i\gamma_4 (1-z_3)}}{1 + R_{45} e^{2i\gamma_4 (1-z_3)}}) S_0(z_3) - S_0'(z_3)], \tag{41.4}$$

$$m_{22} = [i\gamma_4 (\frac{1 - R_{45} e^{2i\gamma_4 (1-z_3)}}{1 + R_{45} e^{2i\gamma_4 (1-z_3)}}) S_1(z_3) - S_1'(z_3)], \tag{41.5}$$

$$f_1 = \frac{-2i\gamma_2 T_{12} e^{-i\gamma_2 z_2}}{R_{21} + e^{-2i\gamma_2 z_2}} \tag{41.6}$$

and the reflection and transmission coefficients are

$$R_{ij} = \frac{\gamma_i - \gamma_j}{\gamma_i + \gamma_j} \qquad \text{and} \qquad T_{ij} = \frac{2\gamma_i}{\gamma_i + \gamma_j}, \tag{42}$$

respectively. If both media 1 and 2 have similar dielectric properties and media 4 and 5 have similar dielectric properties, then $\gamma_1 = \gamma_2$, $\gamma_4 = \gamma_5$, $T_{12} = 1$, $R_{21} = 0$ and $R_{45} = 0$ and the solution in region 3 reduces to the single-layer series solution obtained earlier.

2.5. Finite-element solutions

In order to study the complete heat-transfer problem coupled with the electric-field equations, we solve the electric field and the heat-conduction equations using the Galerkin finite-element method. In this manuscript we only analyze the single-layer situation shown in Figure 1. Since the details of the method have been given elsewhere [4, 9] we only present the basic form of the governing equations and some specific details. Defining the complex field intensity as $u = v_x + iw_x$ the equation for the electric fields, obtained by equating the real (v_x) and imaginary (w_x) components in Equation (17) are

$$\frac{d^2 v_x}{dz^2} + \psi v_x - \chi w_x = 0 \tag{43}$$

and

$$\frac{d^2 w_x}{dz^2} + \chi v_x + \psi w_x = 0\ , \tag{44}$$

where $\psi = \frac{L^2\omega^2}{c^2}\kappa'(s_o)$ and $\chi = \frac{L^2\omega^2}{c^2}\kappa''(s_o)$. The boundary conditions for the real and imaginary components from Equations (8) and (9) are:

$$\left.\begin{aligned} \frac{\mathrm{d}v_x}{\mathrm{d}z} - \gamma_0 w_x &= 0 \\ \frac{\mathrm{d}w_x}{\mathrm{d}z} + \gamma_0 v_x &= 0 \end{aligned}\right\} \quad \text{at} \quad z = 0 \tag{45}$$

and

$$\left.\begin{aligned} \frac{\mathrm{d}v_x}{\mathrm{d}z} + \gamma_0 w_x &= 0 \\ \frac{\mathrm{d}w_x}{\mathrm{d}z} - \gamma_0 v_x &= 0 \end{aligned}\right\} \quad \text{at} \quad z = 1\ . \tag{46}$$

Using ρ_0, $C_{p,0}$ and k_{T0} as the reference thermal properties, the transient $1D$ heat-conduction equation for a slab, Equation (13), is

$$\overline{\rho C_p}\frac{\partial\theta}{\partial\tau} = \frac{\partial}{\partial z}\left(\overline{k_T}\frac{\partial\theta}{\partial z}\right) + P(z)\ , \tag{47}$$

where the expression for the microwave-power term in Equation (47) is,

$$P(z) = \frac{L^2\omega\epsilon_0\kappa''(s_o)E_L^2}{k_{T0}T_0}\left(v_x^2 + w_x^2\right) \tag{48}$$

and

$$\theta = \frac{T - T_\infty}{T_0}\ ,\ \tau = \frac{\alpha_0 t}{L^2}\ , P = \frac{pL^2}{k_{T0}\ T_0}\ ,\quad \overline{\rho C_p} = \frac{(\rho C_p)_{\text{eff}}}{\rho_0\ C_{p,0}} \quad \text{and} \quad \overline{k}_T = \frac{k_{T,\text{eff}}}{k_{T0}}\ ;$$

h is the convection-heat-transfer coefficient, and T_0 is the initial temperature of the material. The boundary conditions are

$$\frac{\partial\theta}{\partial z} - B\mathrm{i}\theta = 0 \ \text{ at } \ z = 0\ , \tag{49}$$

and

$$\frac{\partial\theta}{\partial z} + B\mathrm{i}\theta = 0 \ \text{ at } \ z = 1\ , \tag{50}$$

where $B\mathrm{i} = \frac{hL}{k_{T,\text{eff}}}$ and the initial condition

$$\theta\,(\tau = 0) = \frac{T_0 - T_\infty}{T_0} \quad \text{for} \quad 0 \le z \le 1. \tag{51}$$

For a general equation of the form:

$$Lu = f\ , \tag{52}$$

The finite-element method consists of expanding the unknown, u, in a finite-element basis set Φ. Thus,

$$u \approx \tilde{u} = \sum_{j=1}^{N} u_j \Phi_j(z)\ . \tag{53}$$

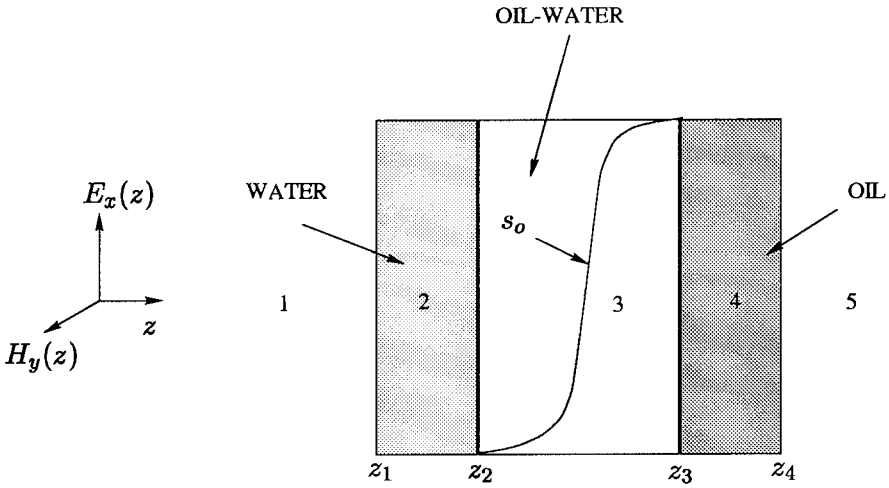

Figure 2. Schematic of multilayered system where the region 2 is saturated with water and region 4 is saturated with oil. The oil saturation s_o varies in region 3.

Table 1. Thermal and dielectric properties for computations reported in this manuscript.

Material	C_p (J kg^{-1} K^{-1})	ρ (kg m^{-3})	k_T (W m^{-1} K^{-1})	κ'	κ''	λ_m (cm)	D_p (cm)
Water	4186·51	1000	0·609	79·5	9·6	1·36	3·6
Oil	2093·26	934	0·168	2·0	0·15	8·64	36·7
Rock	1046·63	2650	0·076	2·8	0·196	–	–
Beef	–	–	–	43	15	1·70	1·80

In the Galerkins method, the error, $L\tilde{u} - f$, is set orthogonal to the basis functions, and

$$\int_0^1 (L\tilde{u} - f)\, \Phi_i dz = 0 \text{ for } i = 1 \ldots N \,. \tag{54}$$

Integrating by parts, and incorporating boundary and interface conditions, we have that Equation (54) results in a set of algebraic equations whose solution yields the unknown coefficients, u_j, of the expansion. Since the dielectric properties are independent of temperature and vary only spatially, the electric-field equations can be solved independent of the heat-transfer equations for this case.

3. Results and Discussion

Table 1, lists the values of the dielectric and thermal properties used in this study. The literature sources for the properties are the following: Thermal and dielectric properties for water and oil [10], thermal properties for rock [2], dielectric properties for rock [12, pp. 79] and dielectric properties for beef [7]. For all the results illustrated in this manuscript we carry out computations for the configuration shown in Figure 1, where the sample is surrounded by free space. Fifty quadratic elements were used for the finite-element computations reported in this manuscript. Initially we compared the series solutions along with the finite-element and analytical solutions, primarily to test the robustness the series solutions. It is well known that

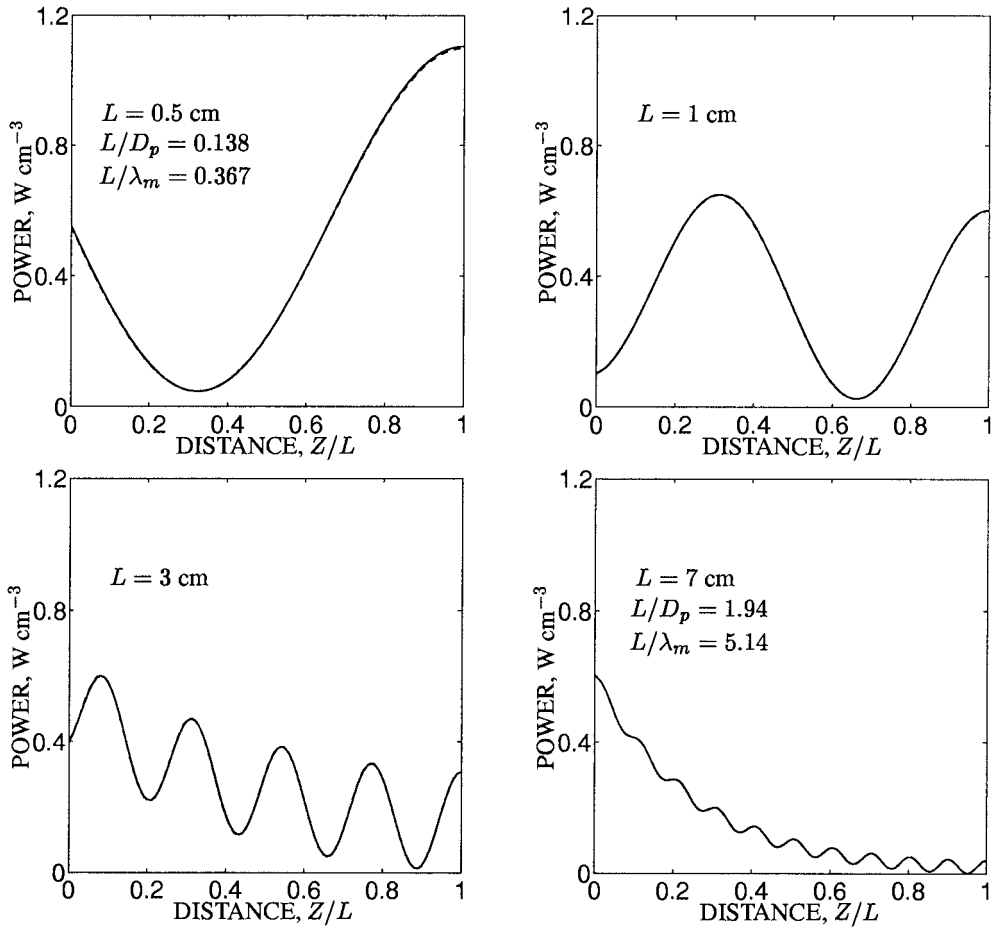

Figure 3. Comparison of series (dashed line) and finite element (solid line) solutions for water with constant dielectric properties.

alternating series, although convergent analytically, can be poorly behaved when evaluated numerically [11, pp 368–378].

Figures 3 and 4 illustrate the series solutions along with the finite-element solution for pure water and oil, respectively, with constant dielectric properties. For water (Figure 3) the power was evaluated for samples with lengths varying from 0.5–7 cm. In this range the L/D_p ratios vary from 0·138 to 1·94. In all situations the comparison is excellent; however the series solution begins to deviate from the finite-element solution for sample lengths greater than about 8 cm ($L/D_p = 2{\cdot}22$). The behaviour in the case of oil (Figure 4) is similar and the series solutions begin to deviate from the finite-element solution for lengths greater than about 50 cm ($L/D_p = 1{\cdot}36$). We also evaluated the solution for a high-loss material, with properties typical of a meat sample. These results, shown in Figure 5 for beef, illustrate that the series solution works well, even for $L/D_p = 4{\cdot}44$.

Our tests with the series solutions illustrate that the convergence of the series solutions improves and solutions at higher L/D_p ratios can be obtained for samples with greater loss tangents. This is clearly observed for the meat sample (Figure 5) where the series solutions work well into the Lambert–law regime, where the power decays exponentially into the sam-

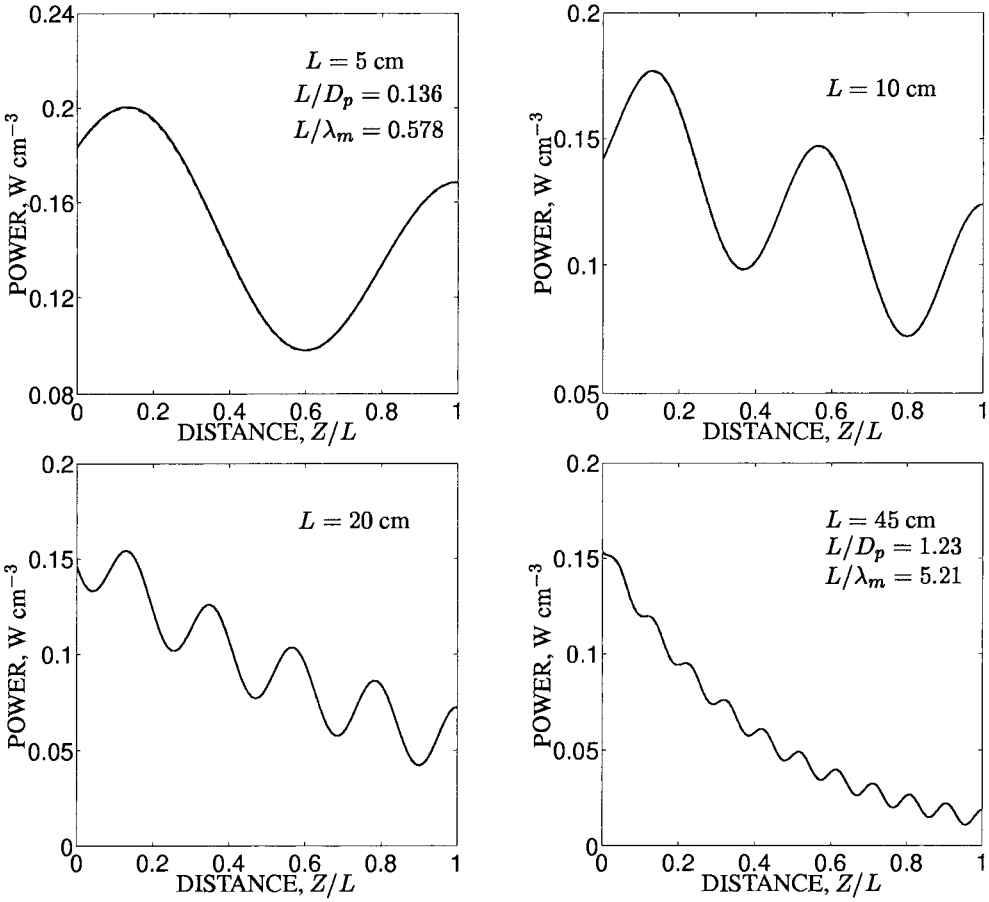

Figure 4. Comparison of series (dashed line) and finite element (solid line) solutions for oil with constant dielectric properties.

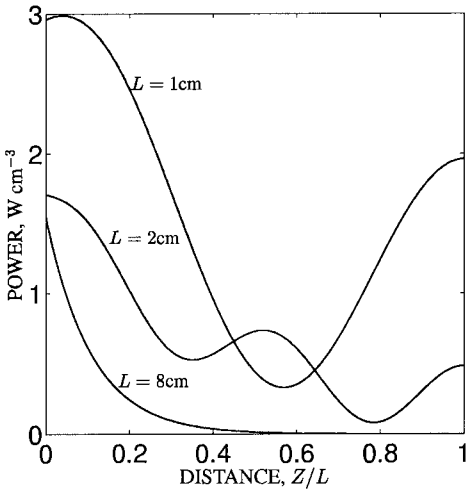

Figure 5. Comparison of series (dashed line) and finite element (solid line) solutions for beef with constant dielectric properties. The series solution works for $L/D_p = 4{\cdot}44$, well into the regime where the absorbed power can be approximated by Lambert's law.

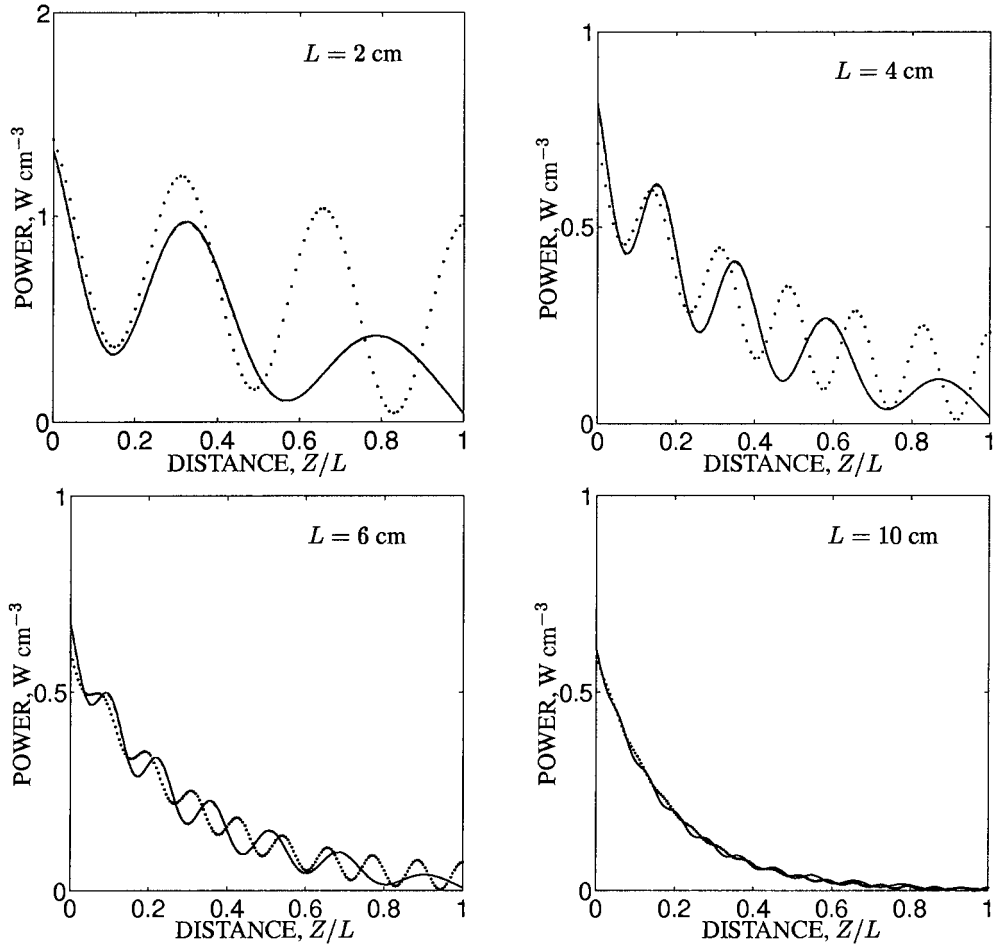

Figure 6. Comparison of series (dashed) and finite-element solutions (solid) for a binary mixture of oil and water assuming a linear variation in the dielectric properties, from pure water at $z = 0$ to pure oil at $z = 1$. The dotted lines which represent the power distribution assuming a pure water sample indicate that the power absorption is dominated by water as the sample thickness increases.

ple. The convergence of the series is significantly faster for smaller samples and the number of terms that must be included in the series increases as the sample thickness is increased. A maximum of 200 terms was used in the results presented. We also found that numerical accuracy played an important role. For example, with double precision, the accurate solutions were obtained only for $L/D_p = 1$; however, with quadruple precision accurate solutions could be obtained for twice the sample lengths. Since we were able to obtain accurate solutions for sample thicknesses where the Lambert–law regime can be used to predict the power, we did not pursue other summation techniques that can potentially improve the accuracy of the series summation [11, pp. 368–378].

Figure 6 illustrates the microwave power distributions for an oil-water mixture, where the dielectric properties vary linearly within the sample, from pure water at $z = 0$ to pure oil at $z = 1$. Since water is the strongly absorbing component, we also compared the power distributions obtained for a pure water sample (dotted lines). The series solutions have been compared with the finite-element solutions for $L = 6$ cm, above which the series solution

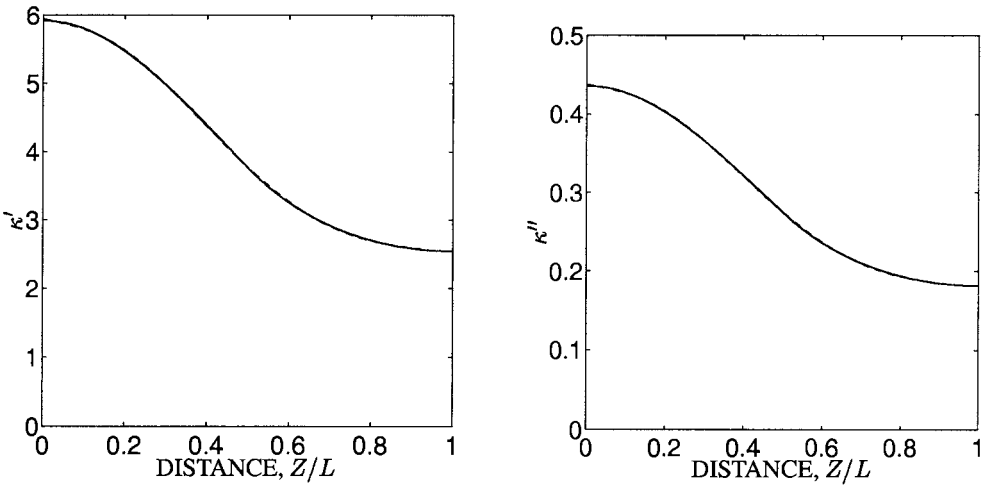

Figure 7. Variation in dielectric properties in the three-phase system of oil, water and rock. The dielectric properties were obtained using Equation 11. First the dielectric properties are obtained for the oil-water mixture assuming that oil forms the continuous phase. Next the dielectric properties of the three-phase system are obtained using the dielectric properties of the oil-water mixture and treating rock as the continuous phase. The dashed line represents the least-squares fit to the dielectric properties using a sixth-order polynomial. The coefficients for the fits are $c_0 = 5{\cdot}93733$, $c_1 = -1{\cdot}16605$, $c_2 = 1{\cdot}24631$, $c_3 = -55{\cdot}6798$, $c_4 = 125{\cdot}126$, $c_5 = -100{\cdot}437$, $c_6 = 28{\cdot}5056$ for κ_2' and $d_0 = 0{\cdot}437738$, $d_1 = -0{\cdot}0892565$, $d_2 = 0{\cdot}119878$, $d_3 = -4{\cdot}25507$, $d_4 = 9{\cdot}37469$, $d_5 = -7{\cdot}53119$, $d_6 = 2{\cdot}12382$ for κ_2''.

begins to lose accuracy. It is interesting to note that a pure-water sample provides an excellent approximation to the power distribution for larger samples. For smaller samples the agreement at the incident face, where the absorption is dominated by water, is better. The presence of oil contributes to the longer wavelengths of the absorbed power in the sample. At $L = 6$ cm and above, although the absorbed power shows the same degree of decay into the sample, the longer wavelength oscillations in the oil-water sample are clearly observed.

We next present electric-field and temperature distributions for the three-phase system of oil, water and rock. If the dielectric properties of the rock and the oil-water mixture are used and a porosity of 0·3 is assumed, the spatial variation of the dielectric properties as a function of the sample length are given in Figure 7. The least-squares fit for the dielectric properties using a sixth-order polynomial are also illustrated in the figure and the coefficients of the polynomial are given in the figure caption. Since the dielectric properties of oil and rock are significantly smaller than that of water (Table 1), the dielectric loss is quite low when compared with that of water. In all the heating computations we have used a low-heat-transfer coefficient of $h = 2$ W m^{-1} K^{-1}.

Figures 8 and 9 illustrates the power distributions and temperature distributions for the oil, water and rock system for samples of varying length. In all cases, excepting the $L = 45$ cm case, the sample was heated for a period of 1 minute. We also compared the power distributions and corresponding heating patterns for a linear variation in the dielectric properties across the sample. We obtained the linear variation using the values of κ' and κ'' at the boundaries of the sample (Figure 7). In addition, the power distributions for the $L = 0{\cdot}5$ cm and 4 cm samples obtained using the sixth-order polynomial fit (Figure 7) for the dielectric properties are also illustrated. We were unable to obtain the series solution with the sixth-order polynomial at larger sample widths due to poor convergence of the series. An excellent

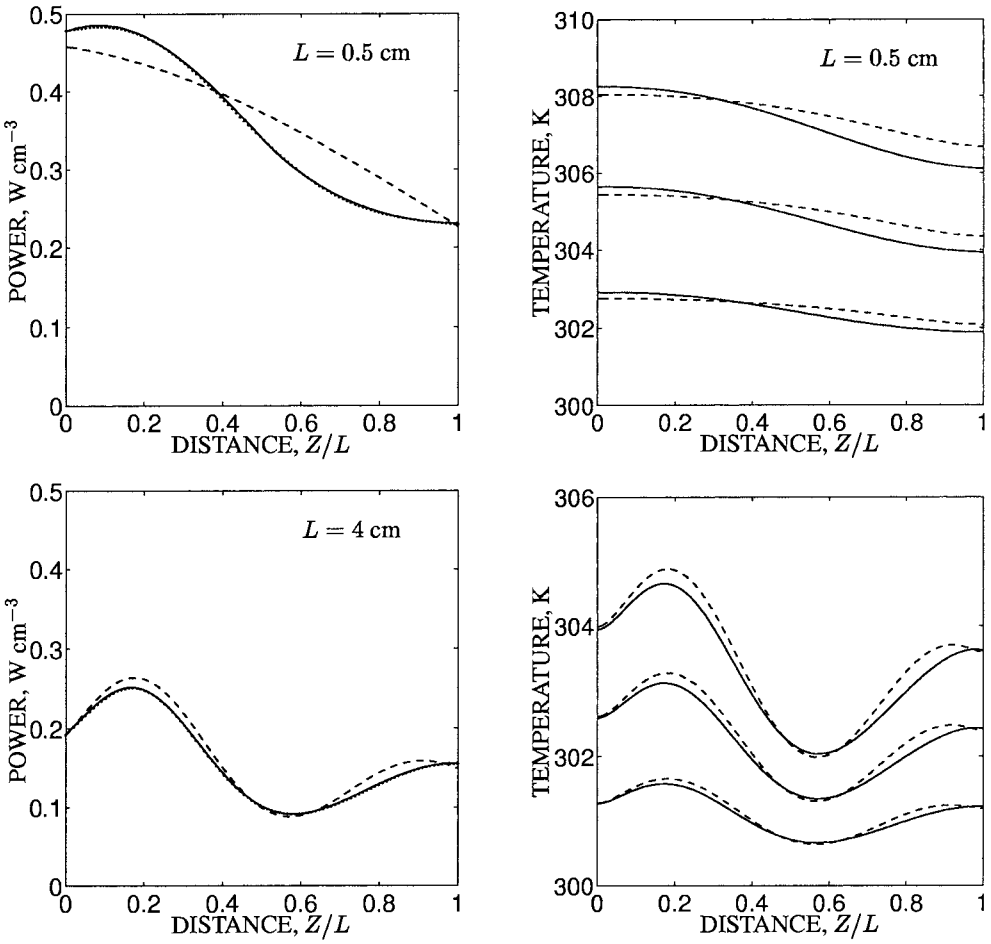

Figure 8. Power and temperature distributions for oil, water and rock system from the finite-element method. The dashed lines are the power and temperature distribution obtained by assuming a linear variation in the dielectric properties. In all cases the total heating time is one minute and temperature distributions are shown at intervals of 20 s. The dotted lines represent power distributions obtained from the series solution using a sixth-order polynomial to fit the dielectric properties shown in Figure 7.

match is observed between the power obtained from the finite-element solution and the series solution for the sixth-order polynomial representation of the dielectric properties. The overall magnitude of the absorbed power is similar to that observed in the pure oil samples (Figure 4). In general, heating is seen to occur at the incident face of the sample due to the larger fraction of water present. Since the saturation of water drops sharply beyond the midpoint of the sample, the temperature distributions clearly reveal a preferential heating in the first half of the sample. However, the low dielectric loss permits heating in the oil-rich regions, as well for the smaller samples. At the largest sample studied ($L = 45$ cm), the power exponentially decays into the sample and heating occurs mainly in the water-rich regions. The difference between the power and temperature distributions and between the actual dielectric property variation and the linear approximation is very good, with the least difference observed for the largest sample studied. In these situations we can obtain the electric field independently using a series solution.

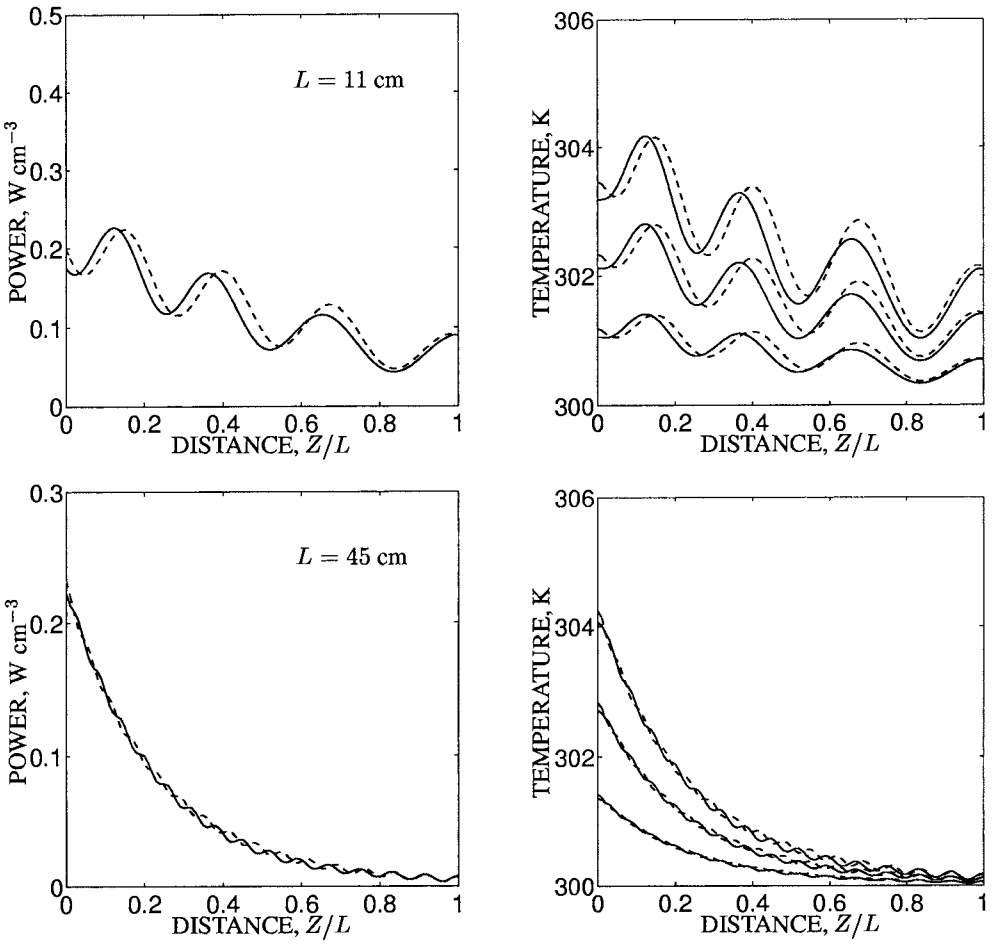

Figure 9. Power and temperature distributions for oil, water and rock system from the finite-element method. The dashed lines are the power and temperature distribution are obtained by assuming a linear variation in the dielectric properties. In all cases, excepting the $L = 45$ cm sample, the total heating time is one minute and temperature distributions are shown at intervals of 20 s. For $L = 45$ cm the total heating time is 3 minutes and the temperature distributions are shown at intervals of 1 minute.

4. Conclusion

We have studied the microwave-power and temperature distributions in samples with spatially varying dielectric properties. Series solutions for the electric field are obtained for situations where the spatial variation of the dielectric properties can be represented by a polynomial. For more general functional forms the solution is obtained by a finite-element solution. The series solution was used to obtain solutions for materials with constant properties and in situations where a linear variation in the dielectric property was assumed. In situations where the dielectric properties vary linearly the power absorption is dominated by the more absorptive component. Our calculations show that for oil-water with a linear variation in dielectric properties varying from pure water to pure oil across the sample, for samples whose thickness exceeds about twice the penetration depth of water, the power distribution is similar to that obtained for a pure-water sample.

Computations where the oil saturation varies in a sigmoidal manner, similar to situations during a water flood to displace oil, across the sample indicate that most of the power absorption occurs in the water-rich regions. In these situations the dielectric properties vary nonlinearly across the sample, with the properties dominated by that of the rock, resulting in a low-loss sample. In these cases we observe the power distribution and heating from a linear variation in the dielectrics is very similar to that obtained using the exact nonlinear forms. Our analysis indicates that, if the dielectric property variation can be represented by a polynomial, the absorbed power can be accurately evaluated, provided the convergence of the series is not a limiting factor.

Although we have analyzed a preliminary laboratory-scale model for microwave heating in a porous rock containing oil and water, a complete engineering analysis would involve investigating the effects of frequency, rate of heating, dynamical evolution of the front and its effect on the overall increase in oil production at the length scales and saturation distributions typically encountered during a water flood. These extensions are currently in progress.

5. Acknowledgement

One of us (KGA) would like to thank S. Kulkarni for helpful discussions during the preparation of this manuscript.

References

1. F. E. Vermeulen and B. McGee, In situ electromagnetic heating for hydrocarbon recovery and environmental remediation. *J. Canad. Petr. Technol.* 39 (2000) 24–28.
2. M. Y. Soliman, Approximate solutions for flow of oil heated using microwaves. *J. Petr. Sci. Eng.* 18 (1997) 93–100.
3. R. E. Collins, *Flow of Fluids through Porous Materials*. New York: Reinhold Publ. Corp. (1961) 270 pp.
4. K. G. Ayappa, H. T. Davis, E. A. Davis and J. Gordon, Analysis of microwave heating of materials with temperature dependent properties. *AIChE J.* 37 (1991) 313–1667.
5. H. Fricke, The complex conductivity of a suspension of stratified particles of spherical or cylindrical form. *J. Phys. Chem.* 56 (1955) 168–174.
6. X. Zeng and A. Faghri, Experimental and numerical study of microwave thawing heat transfer of food materials. *ASME Trans. J. Heat Transfer* 116 (1994) 446–455.
7. K. G. Ayappa, H. T. Davis, G. Crapiste, E. A. Davis and J. Gordon, Microwave heating: An evaluation of power formulations. *Chem. Eng. Sci.* 46 (1991) 1005–1016.
8. E. D. Rainville, *Elementary Differential Equations*. New York: Macmillan (1965) 521 pp.
9. T. Basak and K. G. Ayappa, Analysis of microwave thawing of slabs with effective heat capacity method. *AIChE J.* 43 (1997) 1662–1667.
10. S. A. Barringer, K. G. Ayappa, J. Gordon, E. A. Davis and H. T. Davis, Power absorption during microwave heating of emulsions and layered systems. *J. Food Sci.* 60 (1995) 1132–1136.
11. C. M. Bender and S. A. Orszag, *Advanced Mathematical Methods for Scientists and Engineers*. New York: Mc-Graw Hill (1984) 593 pp.
12. C. A. Balanis, *Advanced Engineering Electromagnetics*. New York: John Wiley & Sons (1989) 981 pp.